AMERICAN SOCIETY FOR MICROBIOLOGY | mBio®

RESEARCH ARTICLE
Host-Microbe Biology

The Role of IgG Subclass in Antibody-Mediated Protection against Carbapenem-Resistant *Klebsiella pneumoniae*

Michael P. Motley,[a,b] Elizabeth Diago-Navarro,[a] Kasturi Banerjee,[a,c] Sean Inzerillo,[a] Bettina C. Fries[a,b,c]

[a]Department of Medicine, Infectious Disease Division, Stony Brook University, Stony Brook, New York, USA
[b]Department of Microbiology and Immunology, Stony Brook University, Stony Brook, New York, USA
[c]Veteran's Administration Medical Center, Northport, New York, USA

ABSTRACT Monoclonal antibodies (MAbs) have the potential to assist in the battle against multidrug-resistant bacteria such as carbapenem-resistant *Klebsiella pneumoniae* (CR-*Kp*). However, the characteristics by which these antibodies (Abs) function, such as the role of antibody subclass, must be determined before such modalities can be carried from the bench to the bedside. We performed a subclass switch on anticapsular monoclonal murine IgG_3 ($mIgG_3$) hybridomas and identified and purified a murine IgG_1 ($mIgG_1$) hybridoma line through sib selection. We then compared the ability of the $mIgG_1$ and $mIgG_3$ antibodies to control CR-*Kp* sequence type 258 (ST258) infection both *in vitro* and *in vivo*. We found by enzyme-limited immunosorbent assay (ELISA) and flow cytometry that $mIgG_3$ has superior binding to the CR-*Kp* capsular polysaccharide (CPS) and superior agglutinating ability compared to $mIgG_1$. The $mIgG_3$ also, predictably, had better complement-mediated serum bactericidal activity than the $mIgG_1$ and also promoted neutrophil-mediated killing at concentrations lower than that of the $mIgG_1$. In contrast, the $mIgG_1$ had marginally better activity in improving macrophage-mediated phagocytosis. Comparing their activities in a pulmonary infection model with wild-type as well as neutropenic mice, both antibodies reduced organ burden in a nonlethal challenge, regardless of neutrophil status, with $mIgG_1$ having the highest overall burden reduction in both scenarios. However, at a lethal inoculum, both antibodies showed reduced efficacy in neutropenic mice, with $mIgG_3$ retaining the most activity. These findings suggest the viability of monoclonal Ab adjunctive therapy in neutropenic patients that cannot mount their own immune response, while also providing some insight into the relative contributions of immune mediators in CR-*Kp* protection.

IMPORTANCE Carbapenem-resistant *Klebsiella pneumoniae* is an urgent public health threat that causes life-threatening infections in immunocompromised hosts. Its resistance to nearly all antibiotics necessitates novel strategies to treat it, including the use of monoclonal antibodies. Monoclonal antibodies are emerging as important adjuncts to traditional pharmaceuticals, and studying how they protect against specific bacteria such as *Klebsiella pneumoniae* is crucial to their development as effective therapies. Antibody subclass is often overlooked but is a major factor in how an antibody interacts with other mediators of immunity. This paper is the first to examine how the subclass of anticapsular monoclonal antibodies can affect efficacy against CR-*Kp*. Additionally, this work sheds light on the viability of monoclonal antibody therapy in neutropenic patients, who are most vulnerable to CR-*Kp* infection.

KEYWORDS antibody therapy, monoclonal antibodies, isotype, carbapenem-resistant *Klebsiella pneumoniae*, antibiotic resistance, *Klebsiella*, antibody function

Monoclonal antibodies (MAbs) are becoming increasingly important in the treatment of a variety of different diseases, including infectious disease (1, 2). The escalating failure of traditional antibiotics to treat bacterial infections further empha-

Citation Motley MP, Diago-Navarro E, Banerjee K, Inzerillo S, Fries BC. 2020. The role of IgG subclass in antibody-mediated protection against carbapenem-resistant *Klebsiella pneumoniae*. mBio 11:e02059-20. https://doi.org/10.1128/mBio.02059-20.

Editor Victor J. Torres, New York University School of Medicine

Address correspondence to Bettina C. Fries, bettina.fries@stonybrookmedicine.edu.

This article is a direct contribution from Bettina C. Fries, a Fellow of the American Academy of Microbiology, who arranged for and secured reviews by Frank DeLeo, National Institute of Allergy and Infectious Diseases, National Institutes of Health, and Tom Kozel, University of Nevada.

Received 24 July 2020
Accepted 28 July 2020
Published 8 September 2020

sizes the importance of testing alternative therapies, including MAbs, against these pathogens (3). Much information regarding how antibody (Ab) structure influences interactions with pathogens remains to be discovered, and until recently the role of the Ab constant region and its different variants, or subclasses, had often been overlooked in therapeutic monoclonal Ab development. While four subclasses of IgG Abs exist in humans, the majority of MAbs used in the clinic are human IgG1 ($hIgG_1$), the most prevalent subclass (4). The subclass of an Ab (dictated by the number of disulfide bonds joining the heavy chains), its fragment crystallizable (Fc) region, and other aspects of the heavy chain, affect what immune receptors and adaptors the antibody binds. Subsequently, these interactions determine the amplitude and character of the immune response (5). Some subclasses interact with more immunostimulatory Fc receptors on professional phagocytes, increasing their activity, while others bind to immunosuppressing receptors that act to reduce collateral damage caused by excessive inflammation (6). Additionally, subclasses can be responsible for differences in antigen binding, even when Abs have identical variable regions (7, 8). Understanding differences between IgG subclasses—how they bind, interact with the pathogen, and interact with other facets of immunity—is important to understanding which subclasses may provide a therapeutic benefit (8–12).

With the recent rise of multidrug-resistant Gram-negative bacteria, such as carbapenem-resistant *Klebsiella pneumoniae* (CR-*Kp*) (13), several laboratories have been focusing on developing antibodies against these pathogens (3, 14–17). These bacteria frequently infect immunocompromised populations that lack robust innate and adaptive immune responses (18, 19). Therefore, it is crucial to understand not only how different Ab subclasses act against these pathogens but also how they function in the context of immunocompromised states. We recently cloned murine IgG_3 ($mIgG_3$) monoclonal Abs that targeted the capsular polysaccharide (CPS) of *wzi154* CR-*Kp* isolates, which fall within the clade 2 subfamily of the CR-*Kp* sequence type 258 (ST258) clonal group (14). Isolates of this conserved subgroup have been shown to be susceptible to Ab therapy through a variety of *in vitro* modalities such as killing by serum complement and action by neutrophils and macrophages, and such antibodies have been shown to be protective *in vivo* as well (14, 15, 20). We chose one of these, 17H12, to study the effects of switching IgG subclass on anti-*Klebsiella* Ab functionality. We report findings that the parent $mIgG_3$ was superior to the new murine IgG_1 ($mIgG_1$) variant in binding ability, initiation of complement-mediated bactericidal activity by serum, and activation of neutrophil-mediated killing at lower antibody concentrations. Conversely, the new $mIgG_1$ variant slightly outperformed the $mIgG_3$ parent in promoting macrophage-mediated phagocytosis of the bacteria. Finally, our comparison within a pulmonary mouse challenge model shows comparable overall efficacy of both subclasses in reducing bacterial organ burden at both lethal and nonlethal inocula in wild-type mice. Interestingly, efficacy of both antibodies was maintained in neutropenic mice except at the lethal inoculum.

RESULTS

Parent 17H12 $mIgG_3$ variant has superior binding of *wzi154* capsular polysaccharide relative to that of the new subclass switch variant 17H12 $mIgG_1$, despite identical variable regions. We first isolated a $mIgG_1$ variant of the $mIgG_3$ 17H12 hybridoma line by using sib selection followed by fluorescence-activated cell sorting (FACS) and soft agar cloning, which we previously utilized (12). Although we sought to generate all three additional subclasses, only $mIgG_1$ and $mIgG_{2a}$ variants were discovered in our initial screen, and only $mIgG_1$ variants could be enriched by downstream sib selection. The $mIgG_1$ hybridomas were verified to exclusively produce $mIgG_1$, and the sequence of the variable region of the new clone was found to be identical to that of the $mIgG_3$ parent (the characteristics of which have been previously published [14]).

To investigate how subclass switching affected binding, we compared the affinity of the new $mIgG_1$ to that of its parent $mIgG_3$ against the *wzi154* CPS originally used to generate the MAb (14). Analysis by enzyme-limited immunosorbent assay (ELISA)

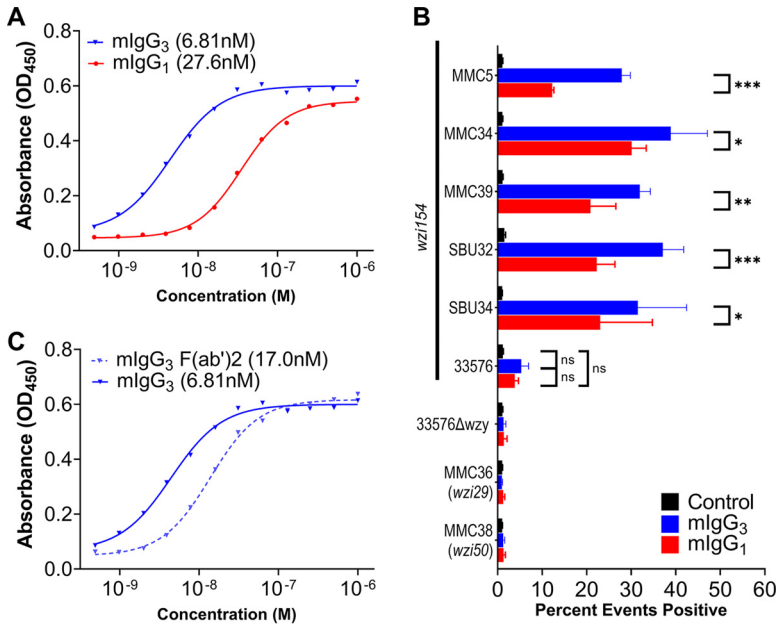

FIG 1 Comparison of binding and agglutination of 17H12 mIgG$_1$ and mIgG$_3$. (A) Binding curves of 17H12 mIgG$_1$ and m17H12 IgG$_3$ measured by indirect enzyme-limited immunosorbent assay (ELISA) on plates coated with *wzi154* (MMC34) capsular polysaccharide (CPS). The 50% effective concentration (EC$_{50}$) values are displayed with legend. The plot is representative of four independent experiments. Differences by unpaired *t* test were determined to be significant ($P = 0.0013$) (B) Relative agglutination of nine CR-*Kp* strains measured by flow cytometry. Agglutination was measured as the percentage of events that exceeded the maximum forward scatter of bacteria without antibody (percent positive). Error bars indicate the standard deviation (SD) from three independent experiments. Two-way analysis of variance (ANOVA) determined a significant difference between treatment groups across strain types ($P < 0.001$), with results of individual comparisons using Tukey's *post hoc* test displayed in the graph. *P* values are replaced with ns (not significant) if $P > 0.1$, * if $P < 0.05$, ** if $P < 0.01$, or *** if $P < 0.001$. (C) Binding curves of 17H12 mIgG$_3$ and its F(ab′)$_2$ fragment, measured by indirect ELISA. The plot is representative of four independent experiments. EC$_{50}$ values are displayed with the legend. Differences between EC$_{50}$ values were determined to be significant by unpaired *t* test ($P < 0.01$).

showed the mIgG$_1$ to have 4-fold less binding than its mIgG$_3$ counterpart, with 50% effective concentration (EC$_{50}$) values of 27.6 nM (95% confidence interval [CI], 18.8 to 40.6 nM) and 6.81 nM (95% CI, 3.00 to 13.2 nM), respectively (Fig. 1A).

Next, we compared the ability of each Ab to agglutinate CR-*Kp* clinical isolates, utilizing flow cytometry to measure relative clump sizes by forward scatter (21). We began testing the Abs with the previously studied CR-*Kp wzi154* strain 39 (MMC39) (14), which we transformed with a novel green fluorescent protein (GFP)-expressing plasmid, pProbe-KtBl. Using this transformant, referred to here as MMC39-GFP, we noted that mIgG$_3$ promoted better agglutination than mIgG$_1$; mIgG$_3$-opsonized bacteria demonstrated higher forward scatter than mIgG$_1$-opsonized bacteria at the same concentration of antibody and also achieved maximum forward scatter at lower concentrations of antibody (see Fig. S1 in the supplemental material). As 30 μg/ml provided the greatest disparity in agglutination between mIgG$_1$ and mIgG$_3$, we chose this antibody concentration and then compared relative agglutination across a number of CR-*Kp* isolates (Table 1). These isolates include those collected from Montefiore Medical Center (MMC) and Stony Brook University (SBU), including those previously studied (14, 22), as well as a previously studied isolate, 33576, from the mid-Atlantic states and its capsule-deficient variant (15) (Table 1). These strains cover the three most prevalent *wzi* subgroups within the ST258 clone (22–24). Measuring the percentage of aggregates larger than a baseline formed by control bacteria untreated with antibody (21), we found that both Abs improved agglutination of nearly all *wzi154* strains relative to that promoted by a control mIgG$_1$ but did not significantly promote agglutination of the capsule-deficient 33576 Δ*wzy* strain or that of CR-*Kp* isolates of the *wzi29* and

TABLE 1 List of CR-*Kp* strains used in the study

Strain	ST	*wzi*	Source of isolate	Reference
MMC5	258	154	Blood isolate from MMC	14
MMC39	258	154	Blood isolate from MMC	14
MMC39-GFP	258	154	Transformant of MMC39	
SBU32	258	154	Urine isolate from SBU	14
SBU34	258	154	Urine isolate from SBU	14
33576	258	154	Isolate from mid-Atlantic	20
33576 Δ*wzy*	258	n/a	Isogenic mutant of 33576	15
MMC36	258	29	Blood isolate from MMC	14
MMC38	258	50	Blood isolate from MMC	14

wzi50 capsule types (Fig. 1B). Additionally, at this concentration the $mIgG_3$ parent caused a higher percentage above baseline of agglutination than that caused by $mIgG_1$ in 5 of 6 isolates. While the percent agglutination of strain 33576 did not significantly improve above baseline for either 17H12 $mIgG_1$ or $mIgG_3$, this was likely due to high observed baseline aggregation of the strain. In contrast, histograms of gated 33576 (and MMC5) demonstrate clear shifts in forward scatter between the $mIgG_3$, $mIgG_1$, and control groups, and aggregated raw mean forward scatter data show significantly higher agglutination by either Ab of all *wzi154* bacteria relative to that in both controls (Fig. S1).

As previous studies have shown the importance of the Fc region in Ab binding to antigen, we performed $F(ab')_2$ digests of both Abs to determine whether this may hold true for 17H12. We determined by ELISA that digestion of 17H12 $mIgG_3$ led to a 2.7-fold loss of binding relative to whole $mIgG_3$ (Fig. 1C). In contrast, digestion of 17H12 $mIgG_1$ did not impact binding (Fig. S2).

Complement-dependent serum killing was exclusive to $mIgG_3$. We next compared the ability of the two subclasses to mediate serum killing of CR-*Kp*. Using 20% fresh human serum, we determined that 17H12 $mIgG_3$ caused 90.1% and 92.7% reductions in CFU of MMC39 CR-*Kp* after 60 and 120 min, respectively. In contrast, the $mIgG_1$ caused 64.4% and 63.5% drops in CFU, respectively, similar to that caused by the control Ab (Fig. 2A). In strain 33576, 20% human serum was found to be insufficient to reduce CFU under any condition (Fig. 2B), but bacterial replication was inhibited by both subclasses, while bacteria exposed to the control multiplied 6-fold over 120 min. Increasing the percentage of serum to 40% improved CFU reduction of the 33576 strain, but in an antibody-independent manner (see Fig. S3 in the supplemental material). As previously described, the 33576 Δ*wzy* strain exhibits pronounced sensitivity to serum in the absence of capsule (15), and nearly complete killing occurred irrespective of treatment (Fig. S3). Variability in killing was observed depending on the human serum donor, but effects were consistent between experiments using serum from the same donor. Additionally, heat inactivation (HI) of serum abrogated all killing effects against MMC39 and instead allowed *K. pneumoniae* growth, which both Abs partially limited (Fig. 2A).

We also specifically compared the relative amount of complement each antibody could fix. Using flow cytometry, we detected C3c and C5b-9 membrane attack complex deposition on MMC39, 33576, and 33576 Δ*wzy* strains in the presence of either subclass (Fig. 2C and D, Fig. S3). We observed the parent $mIgG_3$ to outperform the phosphate-buffered saline (PBS) control and the $mIgG_1$ in deposition of C3c onto MMC39, but not onto 33576, which exhibited high background C3c deposition (Fig. 2C). With both strains, however, C5b-9 deposition was found to be increased when bacteria were preopsonized with $mIgG_3$ (Fig. 2D). Controls confirmed that $mIgG_3$ capsule binding caused deposition of serum-based complement, with incubation of the bacteria in 0% (Fig. 2C and D) or 20% HI serum resulting in no detectable deposition and the antibody failing to deposit additional complement onto the capsule-deficient 33576 Δ*wzy* strain (Fig. S3).

Both subclasses improved macrophage-mediated phagocytosis, with $mIgG_1$ performing marginally better than $mIgG_3$. We next compared the ability of the subclasses to contribute to cell-mediated action against CR-*Kp*. Monocytes and mac-

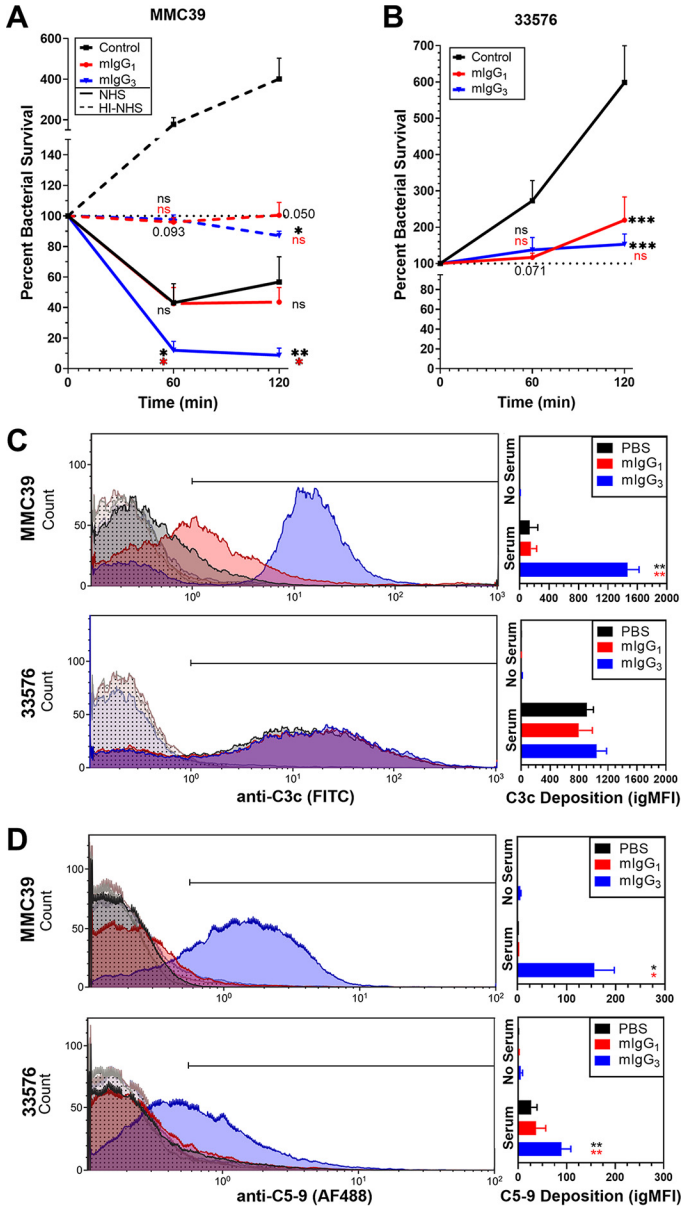

FIG 2 Serum bactericidal effect and complement deposition mediated by 17H12 mIgG$_1$ and mIgG$_3$. (A and B) Growth curves of MMC39 (A) and 33576 (B) in 20% normal human serum (NHS) (both panels, solid lines) or in 20% heat-inactivated (HI)-NHS (panel A only, dashed lines) supplemented with 40 μg/ml of the indicated MAb. "100%" represents no increase in CFU from baseline. Error bars indicate standard error of the mean (SEM) of at least five independent experiments for MMC39 and three for strain 33576. Overall differences between treatment groups in the MMC39 (A) and in 33576 (B) strains were determined to be significant by repeated-measures two-way ANOVA ($P = 0.0380$ and 0.0124, respectively) with results of individual comparisons at 60 min and 120 min using Tukey's *post hoc* test displayed in the graph. (C and D) Fixation of complement components onto strains MMC39 and 33576, as measured by flow cytometry. Left histogram overlays depict representative data from three independent experiments, and right graphs show the means and SEM of the integrated geometric mean fluorescence intensity (igMFI) of each experiment. Histograms of treatments with serum are filled with solid colors, while those without serum have patterned fills. Overall differences between the variances of all treatments for each strain and each complement component were assessed for significance by repeated-measures one-way ANOVA (MMC39 C3c, $P = 0.002$; 33576 C3c $P = 0.228$; MMC39 C5-9 $P = 0.013$; 33576 C5-9 $P = 0.020$) with results of Tukey's *post hoc* test for multiple comparisons displayed in the graph. For all in-graph statistics, *P* values displayed in black are comparisons to the control IgG, whereas *P* values in red compare mIgG$_1$ with mIgG$_3$. *P* values are replaced with ns (not significant) if $P > 0.1$, * if $P < 0.05$, ** if $P < 0.01$, or *** if $P < 0.001$.

rophages are important in CR-*Kp* clearance (25), and we have previously demonstrated 17H12 mIgG$_3$ to enhance phagocytic uptake of numerous *wzi154* CR-*Kp* strains (14). Therefore, we compared the ability of both variants to promote uptake using a CFU-based phagocytosis assay we previously performed (14, 26). Our data show mIgG$_1$ to slightly improve J774A.1 macrophage phagocytosis of MMC39 relative to mIgG$_3$, a trend that was also suggested in the phagocytosis of strain 33576 (Fig. 3A). In contrast, the 33576 Δ*wzy* strain was phagocytosed irrespective of treatment condition. The difference in phagocytosis between mIgG$_1$ and mIgG$_3$ was subtle and was not evident when phagocytosis of MMC39-GFP was observed under fluorescence microscopy (Fig. 3B). Additionally, we found that uptake was not correlated with intracellular killing; after both J774A.1 macrophages and bone marrow-derived macrophages (BMDMs) had phagocytized the opsonized bacteria and external bacteria had been washed away, we observed by both CFU quantitation and by microscopy that the number of bacteria within these cells increased over time (data not shown). This observation suggests intracellular multiplication of CR-*Kp* after phagocytosis.

Neutrophil killing of CR-*Kp* improved with lower concentrations of mIgG$_3$ than mIgG$_1$. We next compared the ability of both antibodies to promote killing by neutrophils. Data in humans has shown that neutropenic patients may have reduced survival in cases of bacteremia caused by CR-*Kp* and other carbapenem-resistant *Enterobacteriaceae* (23). In mice, some studies have shown neutrophils to be important in CR-*Kp* clearance (15, 27), while others have shown them to be less valuable (25). Using a tube-based incubation assay with human neutrophils, we observed both antibodies to promote neutrophil-dependent killing of MMC39 in the presence of 5% autologous serum at 40 μg/ml (Fig. 3C). When we reduced the dose to 10 μg/ml, however, mIgG$_3$ demonstrated improved efficacy, while mIgG$_1$ lost all efficacy relative to that of the control. Antibody-mediated killing by neutrophils was dependent on serum, as coincubation of neutrophils with HI serum failed to reduce bacterial CFU.

We then compared the ability of the two antibodies to promote neutrophil reactive oxygen species (ROS) production in response to CR-*Kp*. We used MMC39, MMC5, SBU32, and SBU34, and either 5% normal human serum (NHS) or 20% HI-fetal bovine serum (FBS) in reactions (Fig. 3D; see also Fig. S4 in the supplemental material). These data indicate that both mIgG$_1$ and mIgG$_3$ promoted ROS production to comparable degrees. However, strains had differing ability to induce ROS production, with strains SBU32 and SBU34 having high constitutive production of ROS in the absence of either monoclonal Ab, whereas base ROS in MMC39 and MMC5 were nearly absent (Fig. 3D, Fig. 4). Furthermore, baseline ROS production in SBU32 and SBU34 occurred irrespective of whether NHS or HI-FBS was used, though NHS appeared to promote marginally higher production.

Both subclasses improved CR-*Kp* lung clearance *in vivo*, including within neutropenic mice. Finally, we compared the protective efficacy of the subclasses *in vivo*, using a pulmonary infection model we previously utilized in BALB/c mice (14). Because we observed these two MAbs to enhance neutrophil-mediated killing, we compared the relative abilities of the subclasses to control organ burden in both c57BL/6 wild-type mice and neutropenic mice, which were generated by Ly6G antibody-mediated depletion. After depleting neutrophils or administering a control Ab, we infected mice with a sublethal dose of MMC39 preopsonized with either the mIgG$_1$, mIgG$_3$, a control mIgG$_1$, or Tris-glycine buffer alone. As we found no significant differences between the mIgG control and the Tris-glycine vehicle, these groups were combined for analysis. We first observed higher CFU lung burden in neutropenic mice, in contrast to observations in previous studies (25, 28). Additionally, we observed efficacy of both subclasses in reducing bacterial burden in the lung in both wild-type and neutropenic mice, with 17H12 mIgG$_1$ having a small but significant advantage over the mIgG$_3$ (Fig. 4A). Additionally, the mIgG$_1$ appeared to promote higher expression of the inflammatory cytokines gamma interferon (IFN-γ), tumor necrosis factor alpha (TNF-α), interleukin-12 (IL-12), and IL-17 in neutropenic mice, suggesting higher im-

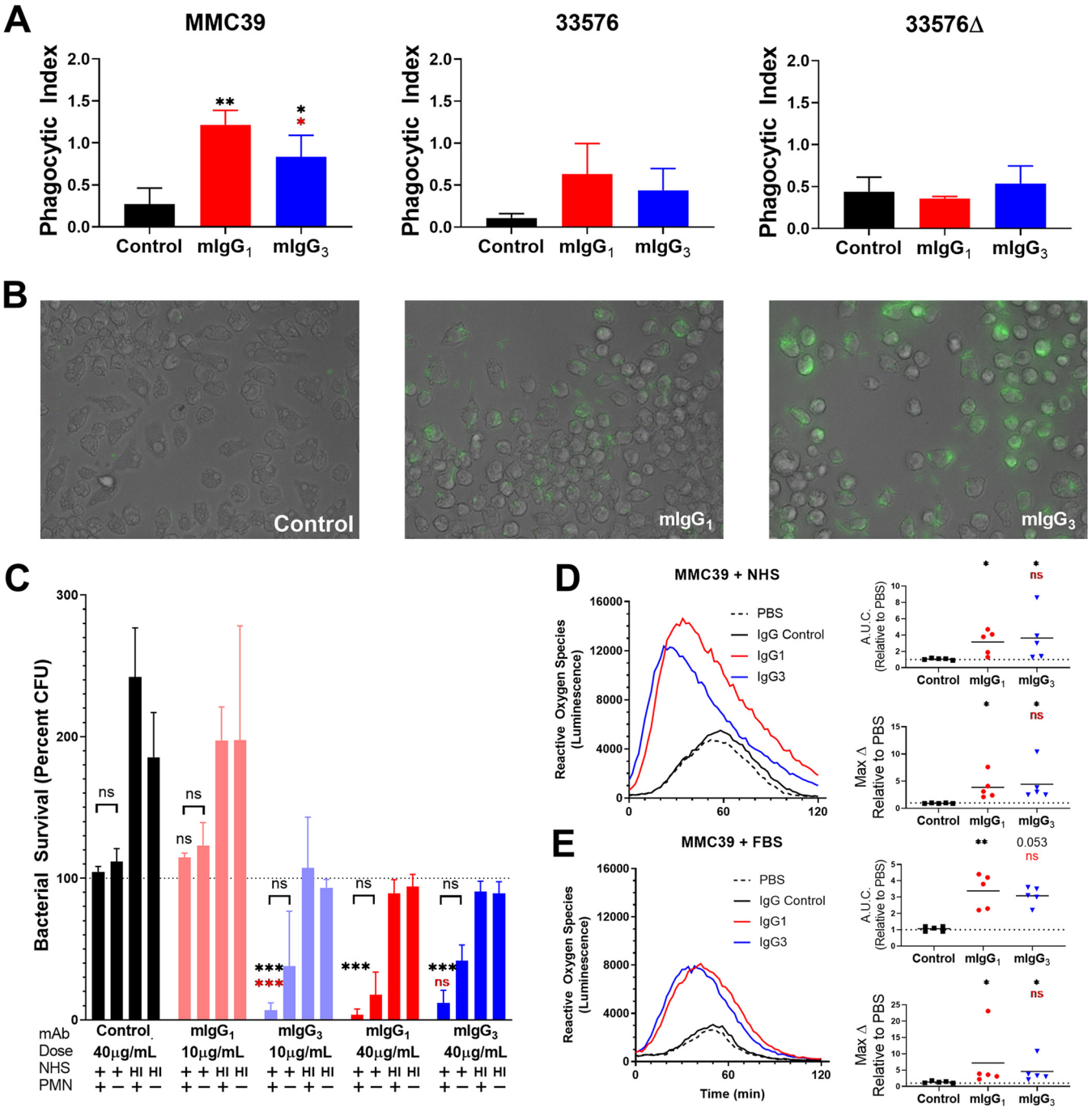

FIG 3 Comparison of cell-mediated phagocytosis and killing. (A) Phagocytosis of the MMC39, 33576, and 33576 Δ*wzy* strains by J774.A1 murine macrophage-like cells after incubation with 40 μg/ml of respective antibody. The phagocytic index is calculated as the number of CFU recovered from the plate, divided by the number of cells plated. Bars depict means and SEMs of three independent experiments, with wells performed in triplicate. Overall differences in the variance of all treatments for each strain were assessed for significance by repeated-measures one-way ANOVA (MMC39 $P < 0.001$; 33576 $P = 0.221$; 33576 Δ*wzy* $P = 0.520$), with results of Tukey's *post hoc* test for multiple comparisons displayed in the graph. (B) Representative images of antibody-mediated phagocytosis of MMC39-green fluorescent protein (GFP) by J774A.1 macrophages. Images were taken at ×40 magnification with an EVOS microscope using brightfield and GFP channels. (C) Killing of preopsonized MMC39 by human neutrophils after 60 min. Bars depict mean and SEM of three independent experiments. Within the results of the NHS-treated samples, differences in the variance of dose-matched treatment groups with and without neutrophils were assessed for significance by two-way repeated-measures ANOVA (variance between treatment groups, $P < 0.001$ for both 10 μg and 40 μg sets; variance comparing neutrophil status, $P = 0.135$ and $P = 0.058$, respectively) with results of Sidak's multiple-comparisons tests displayed in the graph. (D and E) Reactive oxygen species production by human neutrophils exposed to preopsonized MMC39, as measured by luminol luminescence, in the presence of NHS (D) or fetal bovine serum (FBS) (E). The left time lapse graphs are representative of five independent experiments. Right bar graphs show aggregate data of the area under the curve (AUC) and the maximum rate of change (max Δ) relative to those for PBS for all experiments. Differences in AUC and max Δ between control Ab, mIgG$_1$, and mIgG$_3$ were assessed for significance by a Kruskal-Wallis test ($P < 0.01$ for NHS and FBS), with results of Dunn's test for multiple comparisons displayed in the graph. For all in-graph statistics, *P* values displayed in black are comparisons to the control IgG, whereas *P* values in red compare mIgG$_1$ with mIgG$_3$. *P* values are indicated with ns (not significant) if $P > 0.1$, * if $P < 0.05$, ** if $P < 0.01$, and *** if $P < 0.001$.

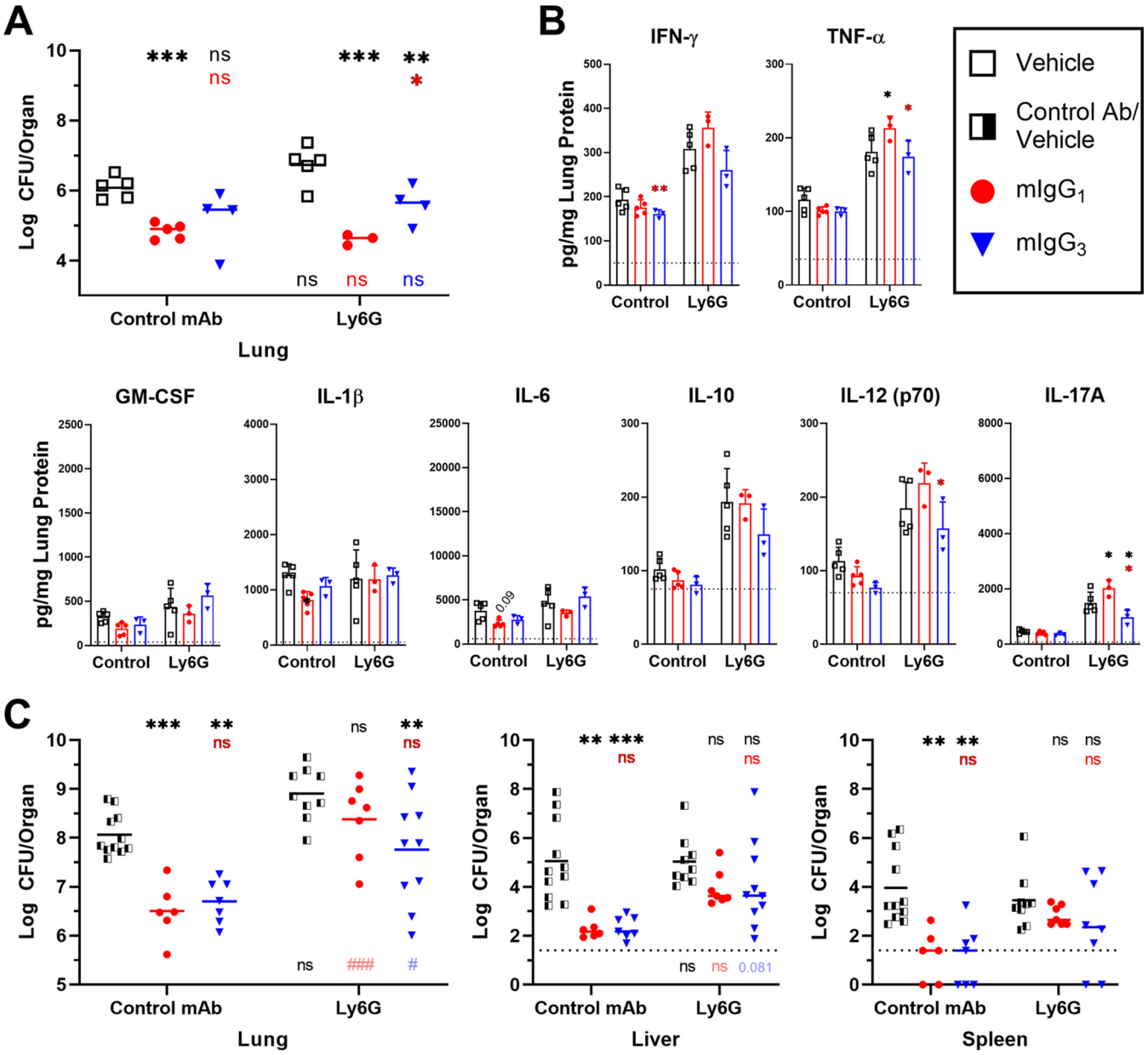

FIG 4 Antibody-mediated protection against CR-*Kp* pulmonary infection in control and neutrophil-depleted mice. (A) Bacterial burden in the lungs of C57BL/6 mice depleted of neutrophils (Ly6G) or administered a control antibody and subsequently infected with a nonlethal inoculum of MMC39 preopsonized with 17H12 subclasses or controls. Each symbol represents one mouse. (B) Cytokine levels, normalized to total lung protein, of mice in panel A, measured by a Bio-Plex panel. (C) Bacterial burden in lungs, liver, and spleen of depleted and nondepleted mice infected with a lethal inoculum of preopsonized MMC39. For all studies, overall differences in CFU and cytokines between treatment groups and between neutrophil status were assessed for significance by two-way ANOVA. Individual comparisons made between treatment groups of mice of the same neutrophil status (* symbols above), or comparisons made between wild-type or neutropenic mice given the same inoculum (# symbols below) were tested using Tukey's *post hoc* test with *P* values displayed in the graph. *P* values are replaced with ns (not significant) if $P > 0.1$, * if $P < 0.05$, ** if $P < 0.01$, or *** if $P < 0.001$. *P* values below plots compare CFU or cytokine levels of wild-type and neutropenic mice within the same treatment group.

mune activation, while the mIgG$_3$ antibody generally exhibited reductions of these markers in neutropenic mice (Fig. 4B).

We proceeded to compare subclass efficacy at a lethal infectious dose, which has been previously observed to cause dissemination to the liver and spleen and death within 72 h. At this dose, both subclasses performed equally in nondepleted mice, reducing lung, liver, and spleen burden by at least 1 log (Fig. 4C). However, within neutropenic mice, mIgG$_1$ showed some loss of efficacy, reducing lung burden by only 0.52 log. Meanwhile mIgG$_3$ continued to reduce burden in all three organs by over 1

log, though results were more variable. Cytokine levels were also more variable as expected, although global increases in inflammatory cytokines such as granulocyte-macrophage colony-stimulating factor (GM-CSF), IL-6, and IL-17 were observed compared to the nonlethal dose (Fig. S4). These cytokines appeared to drop in the presence of either subclass.

Overall, we observed protection of both antibodies in both immunocompetent and neutropenic mice, with a slight advantage of the $mIgG_1$ subclass in mediating small localized infection. At higher doses, both subclasses demonstrated equal efficacy in healthy mice, while only $mIgG_3$ subclass showed significant efficacy in neutropenic mice.

DISCUSSION

Though the pharmaceutical industry has focused primarily on development of $hIgG_1$ antibodies, there are increasing efforts to compare the efficacy of different antibody isotypes and subclasses in treating both cancer and infectious disease (29–31). Despite $mIgG_{2a}$ and $mIgG_{2b}$ being most similar to $hIgG_1$, direct comparisons between $mIgG_1$ and $mIgG_3$ exclusively have provided important insights into antibody-mediated resolution of infection (12, 32, 33). Studies investigating anticapsular antibodies against *Cryptococcus neoformans*, for example, have suggested that $mIgG_3$ is poorly suited to protect against infection compared with $mIgG_1$ (34, 35), whereas protection in mice from *Bacillus anthracis* spores was exclusively mediated by $mIgG_3$ (8). Subclass-specific antibody interactions with *K. pneumoniae* have not been previously studied in detail. Although humoral responses to a CR-*Kp* hexasaccharide vaccine were predominantly $mIgG_1$ (36), $mIgG_3$, like $hIgG_2$, is the primary humoral response to T-independent antigens such as polysaccharide capsules and is the predominant antibody subclass identified after vaccination with full-length capsule (14, 37, 38). This suggests that $mIgG_3$ has some evolutionary importance in protecting against encapsulated organisms.

While having identical variable regions, 17H12 $mIgG_1$ and 17H12 $mIgG_3$ differ in binding the CR-*Kp* capsular polysaccharide, inducing serum bactericidal activity, fixing complement, promoting phagocytosis, and promoting neutrophil-mediated bacterial reduction both *in vitro* and *in vivo*. The improved binding ability of $mIgG_3$ subclasses has been previously observed in antibodies against *Burkholderia* and group A *Streptococcus* capsules (33, 39) and has been attributed to the ability of $mIgG_3$ to self-aggregate, creating opportunities for cooperative binding and increased avidity (40, 41). Our binding and agglutination data extend this knowledge to anticapsular antibodies against CR-*Kp*, although we observed an intermediate level of binding after $F(ab')_2$ digestion of $mIgG_3$, whereas others have observed $mIgG_3$ $F(ab')_2$ fragments to have no better binding than $mIgG_1$ fragments (33, 39). This difference may be due to greater contribution of the $mIgG_3$ hinge region or disulfide bonds to *K. pneumoniae* CPS epitopes (40), and further digestion of the antibody into Fab fragments or replacement of heavy chain domains may shed more light on these interactions (8). Nonetheless, aggregation and cooperative binding appear to be important in defending against encapsulated organisms, since in addition to $mIgG_3$ and cold agglutinin IgM, the T-independent subclass $hIgG_2$ has also demonstrated the ability to self-aggregate (42). Such properties, however, make preparations of monoclonal antibodies exceedingly difficult to purify and store.

Additionally, agglutination of the 33576 strain by our antibodies suggest that clade 2 CPS functional epitopes could be conserved across geographic location. Our previous studies were restricted to *wzi154* clinical isolates collected in the greater New York City area (14, 22). Although further study of the *wzi154* and other ST258 epitopes is warranted, such evidence adds more confidence to efforts to develop cross-protective antibodies and vaccines.

Several studies have shown the resistance of CR-*Kp* strains to serum and the efficacy of antibodies in overcoming this resistance (14, 15, 22, 43). Observing serum bactericidal activity is important when comparing antibody-mediated activity against CR-*Kp*.

Our results reiterate previous findings that $mIgG_3$ Abs promote greater serum killing, as well as C3c and C5b-9 deposition, than $mIgG_1$ Abs can. Fixation of complement by $mIgG_3$ has been shown to be mediated by its CH2 domain (44), and the poor ability of $mIgG_1$ to fix complement has also been observed (45, 46). As previously found and also demonstrated in this study, the capsule is imperative to CR-*Kp* survival in blood (15). Thus, $mIgG_3$ may be more advantageous in limiting CR-*Kp* hematogenous dissemination through complement fixation.

The relative contributions of macrophages, monocytes, and neutrophils to CR-*Kp* clearance has been disputed. While evidence using cell-specific depletions in mice strongly suggested that lung clearance of CR-*Kp* is predominantly mediated by CCR2-positive macrophages over neutrophils (25), studies examining the role of human and primate neutrophils in CR-*Kp* clearance have shown their efficacy in clearing bacteria *in vitro* (15, 27, 47). These contributions matter significantly to the field of anti-infective antibody therapy in the context of CR-*Kp*, as up to 86% of patients with CR-*Kp* bacteremia are neutropenic, and these patients have been found to face worse prognoses than patients without neutropenia (19, 23). Our findings demonstrate that 17H12 $mIgG_1$ may promote improved phagocytosis of CR-*Kp* relative to that promoted by 17H12 $mIgG_3$ in murine J774 cells, as well as similar phagocytosis in bone marrow-derived macrophages. This is interesting, as these antibodies are thought to act via different receptors on the macrophage surface (32, 48). Nevertheless, phagocytosis of two CR-*Kp* strains did not correlate with killing of the bacteria, as CFU and visual evidence indicated that once inside, the CR-*Kp* was able to evade killing by the macrophage, and indeed to multiply within the cell. This phenomenon was also observed previously in non-CR *K. pneumoniae* strains, which were demonstrated to inhibit phagolysosome fusion (49). It is possible that coordination of macrophages with additional immune cells and cytokines in concert may be required for the full capability of antibody-mediated opsonophagocytosis to be realized (50–53). Additionally, alveolar macrophages or inflammatory monocytes may have improved lysosomal capabilities relative to standard BMDMs (54), or macrophages may clear phagocytized bacteria self-destruction via autophagy or pyroptosis (50, 51).

Our studies in human neutrophils showed that $mIgG_3$ promoted better clearance of CR-*Kp* by neutrophils at lower concentrations in the presence of serum. However, while antibody-mediated killing of CR-*Kp* by neutrophils depended on serum, the production of ROS upon stimulation with CR-*Kp* was not, as demonstrated with the production of ROS with heat-killed FBS-enriched media. Such findings suggest that ROS released by neutrophils in response to CR-*Kp* may be reactionary without being protective; further studies examining ROS responses *in vivo*, as well as studies examining other neutrophil protection mechanisms, such as lysosomal activity and neutrophil extracellular trap release, are warranted.

Our *in vivo* data provides several important findings. First, as previously stated, we observed CFU in the lungs of MMC39-infected mice to be higher in the neutrophil-depleted mice in both sublethal and lethal challenges, suggesting that neutrophils are indeed important in protection against pulmonary infection by this *wzi154* isolate. This runs counter to other studies that found no change in CFU in lungs of neutropenic mice (25, 28). Our laboratory has previously discovered variability in the virulence of ST258 strains, including within *wzi154* strains (22), and additional work has determined that neutrophils can clear some ST258 strains (47). Therefore, it is possible that immune responses to different CR-*Kp* strains may differ and thus be responsible for these differences.

Additionally, we observe potential differences in protection by the different subclasses. While both antibodies reduced bacterial burden in the lungs of mice, 17H12 $mIgG_1$ performed better, and the $mIgG_1$ was associated with higher levels of inflammatory cytokines in neutropenic mice than those in the control-treated or $mIgG_3$-treated mice when given a sublethal dose. We suggest that at low inocula, monocytes and macrophages may be more important for infection control, and as $mIgG_1$ showed better opsonophagocytosis, it may function as the better subclass in these mice. As

mentioned, bacterial control by macrophages could be augmented by other immune populations such as gamma delta T cells and innate type III lymphocytes, all of which may produce IL-17 to potentiate *Klebsiella* immunity (28, 55, 56). Increased levels of IL-17, IL-12, and other cytokines in the neutropenic mice may thus compensate for neutrophil responses through action by macrophages, monocytes, and other cells. IL-17, produced by resident lymphocyte populations, has been identified as indispensable in protection against *K. pneumoniae* pulmonary infection (28, 55–58). However, these neutrophil-independent responses may be insufficient at higher inocula, as evidenced by the reduction of $mIgG_1$ efficacy in the neutropenic mice challenged with lethal infection. In contrast, drops in inflammatory cytokines in $mIgG_3$-treated neutropenic mice may indicate that other components, such as complement, may be sufficient to control infection and require fewer compensatory distress cues for local control. Complement has been shown to be important in lung clearance of other pathogens early in infection (59, 60). Furthermore, retention of efficacy by $mIgG_3$ in the high-inoculum neutropenic scenario may suggest a large role of complement in defending against more disseminated infection, when local control of infection by macrophages and other resident populations may be insufficient to compensate for the role of neutrophils. Studying subclass using complement depletion models may provide additional insights into the relative contribution of complement in antibody-mediated protection.

Our study has several limitations. First, large heterogeneity in virulence exists between *K. pneumoniae* isolates, even within CR-*Kp* subsets (22), and our contrasting findings regarding neutrophil protection highlight the need to further study heterogeneity of the pathogen-immune response in numerous CR-*Kp* isolates (25). Furthermore, the functions of individual monoclonal antibodies, even those with the same subclass and similar target, can also be heterogeneous. Some anticapsular *Streptococcus pneumoniae* antibodies are better able to promote opsonophagocytosis, while others may directly interference with bacterial signaling and growth (61, 62). Therefore, future studies of CR-*Kp* anticapsular antibodies should investigate several to better sample their potential. Finally, future studies of anti-CR-*Kp* antibodies must innovate the field of *in vivo* models used to study CR-*Kp* infection, as convenient and effective models that reproduce the chronic, persistent infection caused by CR-*Kp* in humans have been difficult to develop (27).

In conclusion, we find that the subclass differences of an anticapsular antibody can affect various facets of immune function against carbapenem-resistant *Klebsiella pneumoniae* but can exhibit similar efficacy *in vivo*. This information will promote future monoclonal antibody work on CR-*Kp* to provide effective therapies, and supports the potential of antibody 17H12 as a candidate to further study. Furthermore, we observe a role for neutrophils in antibody-mediated protection *in vivo*, encouraging further efforts to investigate the pathogen-host interactions of CR-*Kp*.

MATERIALS AND METHODS

Ethics statement. Animal study protocols were approved by the Animal Committee (IACUC) at Stony Brook University in accordance with the Guide for the Care and Use of Laboratory Animals, the Animal Welfare Act, the Public Health Service Policy on Human Care and Use of Laboratory Animals, and all other local, state and federal regulations. Healthy serum and neutrophil donors gave written informed consent for blood donation under institutional review board (IRB) protocol 718744 at SBU.

Bacteria and growth conditions. *Klebsiella pneumoniae* MMC5, MMC34, and MMC39 are *wzi154* clinical isolates, and MMC36 and MMC38 are *wzi29* and *wzi50* isolates, respectively, from Montefiore Medical Center and were described previously (22). SBU32 and SBU34 are clinical isolates from Stony Brook University Hospital previously used to study 17H12 $mIgG_3$ (14). Strain 33576 and its capsule-deficient mutant (33576 Δ*wzy*) were graciously provided by Barry Kreiswirth (15). For all experiments (unless otherwise noted), strains were grown at 37°C shaking to the mid-exponential phase in Miller LB broth from a 1:100 dilution of an overnight culture. Overnight cultures were derived from single colonies picked from a Miller LB plate no older than 30 days. Unless stated otherwise, cultures were washed with PBS twice before use.

Generation of pProbe-KtBl and transformation of CR-*Kp* MMC39. We previously utilized a pPROBE-Kt GFP plasmid with a pVS1 backbone and with GFP under the control of an inserted *nptII* kanamycin promoter (26, 63). We used this plasmid and, under contract with Genewiz, inserted the sequence of the *sh ble* gene, which conveys resistance to bleomycin, into a ClaI cut site positioned

between the *ori* and the existing *kan*^{r} cassette. Insertion of the gene was confirmed both by sequencing and by digest with BssHII, which both the original pPROBE-Kt and the *sh ble* gene possessed. The plasmid was transformed into MMC39 by electroporation and plated onto Lennox (low-salt) LB with pH adjusted to 8.0 and containing 50 μg/ml bleomycin (Zeocin; Thermo Fisher). Transformation was confirmed by growing positive colonies on 50 μg/ml bleomycin and 50 μg/ml kanamycin and observing GFP fluorescence of selected colonies under a microscope. To test for plasmid stability, we tested replicate plating of 100 unselected colonies onto selective plates, all of which grew. Additionally, nearly all bacteria screened after 10 serial exponential cultures of MMC39 in the absence of antibiotics were shown to be GFP-positive (GFP$^+$) by microscopy. For all later experiments, MMC39-GFP isolates were streaked onto Miller LB agar supplemented with 50 μg/ml of kanamycin and grown in kanamycin-supplemented Miller LB broth.

Subclass switch production and sequencing. The mIgG$_1$ switch variant of the 17H12 mIgG$_3$ murine hybridoma was generated as previously described (12). Briefly, the mIgG$_3$ parent hybridoma line was treated with endotoxin and IL-4, and spontaneous switch variants were identified through enzyme-linked immunosorbent spot (ELISpot). Sib selection was initially utilized, followed by two rounds of fluorescence-activated cell sorting (FACS) of cells stained with fluorescein isothiocyanate (FITC)-conjugated rat anti-mouse IgG$_1$ (catalog no. 1144-02; SouthernBiotech), and by rounds of soft-agar cloning in SeaPlaque agarose. Vials of frozen hybridoma clones were sent to GenScript for variable region exon sequencing and analysis through the IMGT/V Quest program.

Antibody purification. Antibodies were produced weekly over 6 months from respective hybridomas grown in CELLine (Wheaton) flasks fed with high-glucose Dulbecco's modified Eagle's medium (DMEM) plus 10% NCTC medium and 1× penicillin-streptomycin and 1× nonessential amino acids, supplemented with either 10% or 5% FBS in the inner and outer chambers, respectively. These antibodies were purified using Pierce protein G affinity chromatography per the manufacturer's instructions. Eluted antibody was neutralized in Tris-HCl (pH 8.0) and NaCl to final concentrations of 100 mM and 300 mM, respectively, then concentrated by centrifugal filtration (Amicon 30K), filter sterilized, snap-frozen in liquid nitrogen, and stored at −80°C until use. Concentration was determined by absorbance at 280 nM (extinction coefficient = 1.4), which correlated with Bradford assay results.

F(ab′)$_2$ generation. F(ab′)$_2$ fragments of 17H12 mIgG$_3$ and mIgG$_1$ were generated and purified using the Pierce F(ab′)$_2$ preparation kit and mouse IgG$_1$ Fab/F(ab′)$_2$ preparation kits following the manufacturer's instructions, except for digestion temperature and duration (10 min at ambient temperature for mIgG$_3$ and 36 h at 37°C for mIgG$_1$). Coomassie staining of SDS-PAGE in nonreducing conditions was utilized to ensure MAb/F(ab′)$_2$ purity after all purifications/digestions.

Binding affinity. The EC$_{50}$ of the MAbs was calculated using ELISA as described previously (26). Briefly, polystyrene plates (Corning 3690) were coated with 0.5 mg/ml of ST258 clade 2 CPS (MMC34) in PBS, then blocked with 1% PBS-bovine serum albumin (BSA). The MAbs or F(ab′)$_2$ fragments were serially diluted starting at 1 μM [assuming molecular weights (MW) of 150 kDa for full IgG and 110 kDa for F(ab′)$_2$, respectively] and proceeding 2-fold. Antibody was detected using a horseradish peroxidase (HRP)-conjugated goat anti-mouse IgG kappa secondary antibody (1:1,000, catalog no. PA1-86015; SouthernBiotech) and developed with 1-Step Turbo TMB (*N*,*N*,*N*′,*N*′-tetramethyl-1,3-butanediamine) ELISA substrate (Thermo Fisher) according to the manufacturer's instructions. Between steps, wells were washed four times with PBS-0.1% Tween 20. Experiments were repeated on two different days with two different antibody purification batches and digests to ensure reproducibility. Control antibodies were run in parallel as negative controls (catalog no. 0102-01 and 0105-01; SouthernBiotech).

Agglutination. Agglutination of bacteria by MAbs was detected by flow cytometry and confirmed by microscopy, similarly to previous studies (21, 64). Washed cultures were diluted to approximately 1×10^8 CFU/ml, and 40 μl was added to 160 μl of PBS with the appropriate antibody concentration and 0.5% BSA to give a final concentration of 2×10^7 CFU/ml. The samples were mixed gently in round-bottomed flow cytometry tubes and incubated at 37°C in a shake incubator for 1 h, and later fixed by adding 200 μl of 2% paraformaldehyde (PFA) and incubating for 10 min at room temperature (RT). Fixed samples were analyzed via FACSCalibur using forward and side scatter to determine clump sizes and also visualized on glass slides under phase-contrast microscopy (EVOS FL Auto, 40× and 100× objectives; Thermo Fisher). Voltages for flow cytometry were fixed throughout, but gating of bacteria was adjusted based on individual strains incubated in PBS alone to account for size differences between strains. In total, 50,000 events within the gate were counted per sample, representing ~75% of all recorded events. The percentage of positive agglutination events was calculated by measuring the percentage of gated cells whose forward scatter exceeded a value representing the largest 1% of events for bacteria treated with PBS alone. The control antibody utilized, 14G8, was an mIgG$_1$ against *Staphylococcus aureus* enterotoxin B (SEB) (65).

Serum resistance assays. Serum resistance/killing assays were modified from a previously described assay (22). Briefly, 250 μl of a 1×10^5 CFU/ml solution was added to 750 μl of PBS containing 20% fresh or heat-inactivated (HI) human serum from a healthy donor. HI serum was generated from donor serum by a 30-min incubation in a 57°C water bath. Tubes were incubated at 37°C, rotating end over end. At 0, 60, and 120 min after mixing, 100 μl was sampled from each tube, diluted, and plated onto LB agar for CFU quantitation. Percent survival was measured as a fraction of the CFU count at 0 min.

Complement deposition assays. Flow cytometry was used to detect complement deposition of C3c and C5b-9, as previously described (14). Briefly, bacteria were diluted to 1×10^8 CFU/ml in 1 ml PBS-BSA 1% or 20% fresh human serum (in PBS-BSA). PBS or 10 μg/ml of antibody was then added, and bacteria were incubated either 20 min or 40 min at ambient temperature for C3c and C5b-9 deposition, respectively. Bacteria were washed, resuspended in PBS-BSA, and incubated with either

FITC-conjugated sheep anti-human C3 (catalog no. AHP031F; Bio-Rad) at 1:500 or AF488-conjugated mouse anti-C5b-9 (ae11) (catalog no. 5120AF488; Novus Biologicals) at 1:150 or without antibody for 20 min at 4°C. After incubation, bacteria were washed and analyzed for fluorescence by FACSCalibur. Integrated geometric mean fluorescence was measured as the product of the percentage of gated events that passed a fluorescence threshold and the mean fluorescence of those events that passed the threshold.

Macrophage phagocytosis assays. BMDMs were differentiated from frozen bone marrow from 6 week-old c57BL/6 mice (Taconic) as previously described (66), except using pure macrophage colony-stimulating factor (M-CSF) (10 ng/ml) rather than L929 medium as the M-CSF source for feedings on days 1 and 4. Differentiation of cells was confirmed by flow cytometry on cells stained with FITC-conjugated anti-F4/80 and BV510-conjugated CD11b (purity, >98% double positive). Macrophage phagocytosis as measured by CFU was performed similarly to previous protocols (22, 26), Briefly, 1×10^5 BMDM or J774A.1 cells were incubated overnight in wells of cell culture-treated 96-well plates. BMDMs were cultured in RPMI with HEPES and L-glutamine supplemented with 10% FBS and 1× nonessential amino acids, while J774A.1 cells were cultured in DMEM supplemented with 10% FBS, 10% NCTC-109, and 1× nonessential amino acids. The following day, 1×10^7/ml bacteria were opsonized for 20 min in respective cell culture media containing 40 μg/ml of either mIgG$_1$, mIgG$_3$, or control mIgG$_1$, and 100 μl of this (multiplicity of infection [MOI] = 10) was added to each well of the washed macrophage plates. After 30 min of incubation at 37°C in 5% CO_2, cells were washed thrice and exposed to medium with 100 μg/ml of polymyxin B for 20 min. Cells were washed again, and time 0 wells were immediately lysed twice with water and plated, while those at later time points remained in culture medium until needed. All conditions were performed in triplicate wells. The number of CFU calculated from LB plates was divided by the number of estimated cells plated to give the phagocytic index. Microscopy was performed using the MMC39-GFP strain and EVOS FL Auto (40× objective; Thermo Fisher) using phase contrast and a GFP light cube.

Neutrophil killing assays. Neutrophil assays were adapted from a previous protocol (15). Briefly, 5×10^5 bacteria opsonized for 30 min at RT in RPMI medium containing appropriate antibody concentrations were added to 5×10^5 human neutrophils in RPMI medium containing a final concentration of 5% autologous fresh or HI serum. At 0, 15, 30, and 60 min, 100 μl were sampled from reaction tubes, lysed in cold PBS plus 0.1% Triton X-100, diluted in PBS, and plated on LB agar for CFU quantitation. Percent survival was measured as a fraction of the CFU count at 0 min. Tubes containing sera but not neutrophils were run in parallel. Neutrophils were purified from whole blood using a MACSxpress whole blood neutrophil isolation kit (Miltenyi), treated once for 5 min with red blood cell lysis buffer, and resuspended in RPMI medium on ice until use. Flow cytometry performed on neutrophils purified from two experiments both showed a purity pf >99%.

Pulmonary infection experiments. We used c57BL/6 mice (Taconic) aged 7 to 9 weeks for all mouse experiments, and pulmonary infection was performed as previously (14, 67). At 48 and 4 h prior to the procedure, mice were injected intraperitoneally with 225 μg of rat anti-mouse Ly6G (1A8) or a control rat anti-mouse IgG$_{2a}$ (2A3) (BioXcell). Neutrophil depletion was confirmed previously using flow cytometry of lung homogenates (Ly6G$^+$, Ly6C$^-$, CD11b$^-$). Inocula were prepared by resuspending MMC39 in a Tris-glycine buffer containing 5 mg/ml of an ovalbumin control mIgG$_1$ (Crown Biosciences), 17H12 mIgG$_1$, or 17H12 mIgG$_3$ to a final concentration of 6×10^6 or 3×10^7 CFU/ml. After 1 h of opsonization, 50 μl of the inoculum was instilled into the surgically exposed trachea of a mouse under ketamine/xylazine using a bent 27-gauge needle. After 20 h, mice were euthanized, and lungs, liver, and spleen were collected and processed in NP-40 or PBS and diluted to enumerate CFU. Supernatants of lung homogenates used for cytokine analysis were stored at −80°C with 1× Pierce proteinase inhibitor until testing using Bio-Plex Pro mouse cytokine Th17 panel A with additional GM-CSF and IL-12p70 singleplex sets on a Bio-Plex 200 Platform (Bio-Rad). Cytokine levels were normalized against total protein measured by Bradford assay.

SUPPLEMENTAL MATERIAL

Supplemental material is available online only.

FIG S1, TIF file, 1.7 MB.

FIG S2, TIF file, 0.8 MB.

FIG S3, TIF file, 0.7 MB.

FIG S4, TIF file, 0.7 MB.

FIG S5, TIF file, 0.4 MB.

ACKNOWLEDGMENTS

This study was funded using NIAID F30 AI140611 and U.S. Veterans Affairs Merit Review award I01 BX003741.

B.C.F. is an attending at the U.S. Department of Veterans Affairs (VA)—Northport VA Medical Center, Northport, NY. We report no financial conflicts of interest.

The contents of this review do not represent the views of the VA or the United States Government.

We thank Liang Chen and Barry Kreiswirth for gifting us CR-*Kp* strain 33576 and its

acapsular mutant. We also thank Bruna Seco and Peter Seeberger for their initial contributions to the project. Additionally, we thank Anne Savitt for her assistance in editing the manuscript.

REFERENCES

1. Marston HD, Paules CI, Fauci AS. 2018. Monoclonal antibodies for emerging infectious diseases—borrowing from history. N Engl J Med 378:1469–1472. https://doi.org/10.1056/NEJMp1802256.
2. Kaplon H, Muralidharan M, Schneider Z, Reichert JM. 2020. Antibodies to watch in 2020. MAbs 12:1703531. https://doi.org/10.1080/19420862.2019.1703531.
3. Motley MP, Fries BC. 2017. A new take on an old remedy: generating antibodies against multidrug-resistant gram-negative bacteria in a postantibiotic world. mSphere 2:e00397-17. https://doi.org/10.1128/mSphere.00397-17.
4. Irani V, Guy AJ, Andrew D, Beeson JG, Ramsland PA, Richards JS. 2015. Molecular properties of human IgG subclasses and their implications for designing therapeutic monoclonal antibodies against infectious diseases. Mol Immunol 67:171–182. https://doi.org/10.1016/j.molimm.2015.03.255.
5. Lu LL, Suscovich TJ, Fortune SM, Alter G. 2018. Beyond binding: antibody effector functions in infectious diseases. Nat Rev Immunol 18:46–61. https://doi.org/10.1038/nri.2017.106.
6. Nimmerjahn F, Ravetch JV. 2008. Fcγ receptors as regulators of immune responses. Nat Rev Immunol 8:34–47. https://doi.org/10.1038/nri2206.
7. Janda A, Eryilmaz E, Nakouzi A, Cowburn D, Casadevall A. 2012. Variable region identical immunoglobulins differing in isotype express different paratopes. J Biol Chem 287:35409–35417. https://doi.org/10.1074/jbc.M112.404483.
8. Hovenden M, Hubbard MA, Aucoin DP, Thorkildson P, Reed DE, Welch WH, Lyons CR, Lovchik JA, Kozel TR. 2013. IgG subclass and heavy chain domains contribute to binding and protection by MAbs to the poly gamma-D-glutamic acid capsular antigen of *Bacillus anthracis*. PLoS Pathog 9:e1003306. https://doi.org/10.1371/journal.ppat.1003306.
9. Tudor D, Yu H, Maupetit J, Drillet AS, Bouceba T, Schwartz-Cornil I, Lopalco L, Tuffery P, Bomsel M. 2012. Isotype modulates epitope specificity, affinity, and antiviral activities of anti-HIV-1 human broadly neutralizing 2F5 antibody. Proc Natl Acad Sci U S A 109:12680–12685. https://doi.org/10.1073/pnas.1200024109.
10. Torres M, May R, Scharff MD, Casadevall A. 2005. Variable-region-identical antibodies differing in isotype demonstrate differences in fine specificity and idiotype. J Immunol 174:2132–2142. https://doi.org/10.4049/jimmunol.174.4.2132.
11. Yuan RR, Spira G, Oh J, Paizi M, Casadevall A, Scharff MD. 1998. Isotype switching increases efficacy of antibody protection against *Cryptococcus neoformans* infection in mice. Infect Immun 66:1057–1062. https://doi.org/10.1128/IAI.66.3.1057-1062.1998.
12. Varshney AK, Wang X, Aguilar JL, Scharff MD, Fries BC. 2014. Isotype switching increases efficacy of antibody protection against staphylococcal enterotoxin B-induced lethal shock and *Staphylococcus aureus* sepsis in mice. mBio 5:e01007-14. https://doi.org/10.1128/mBio.01007-14.
13. van Duin D, Arias CA, Komarow L, Chen L, Hanson BM, Weston G, Cober E, Garner OB, Jacob JT, Satlin MJ, Fries BC, Garcia-Diaz J, Doi Y, Dhar S, Kaye KS, Earley M, Hujer AM, Hujer KM, Domitrovic TN, Shropshire WC, Dinh A, Manca C, Luterbach CL, Wang M, Paterson DL, Banerjee R, Patel R, Evans S, Hill C, Arias R, Chambers HF, Fowler VG, Kreiswirth BN, Bonomo RA, Multi-Drug Resistant Organism Network Investigators. 2020. Molecular and clinical epidemiology of carbapenem-resistant *Enterobacterales* in the USA (CRACKLE-2): a prospective cohort study. Lancet Infect Dis 20:731–741. https://doi.org/10.1016/S1473-3099(19)30755-8.
14. Diago-Navarro E, Motley MP, Ruiz-Perez G, Yu W, Austin J, Seco BMS, Xiao G, Chikhalya A, Seeberger PH, Fries BC. 2018. Novel, broadly reactive anticapsular antibodies against carbapenem-resistant *Klebsiella pneumoniae* protect from infection. mBio 9:e00091-18. https://doi.org/10.1128/mBio.01005-18.
15. Kobayashi SD, Porter AR, Freedman B, Pandey R, Chen L, Kreiswirth BN, DeLeo FR. 2018. Antibody-mediated killing of carbapenem-resistant ST258 *Klebsiella pneumoniae* by human neutrophils. mBio 9:e00297-18. https://doi.org/10.1128/mBio.00297-18.
16. Ali SO, Yu XQ, Robbie GJ, Wu Y, Shoemaker K, Yu L, DiGiandomenico A, Keller AE, Anude C, Hernandez-Illas M, Bellamy T, Falloon J, Dubovsky F, Jafri HS. 2019. Phase 1 study of MEDI3902, an investigational anti-*Pseudomonas aeruginosa* PcrV and Psl bispecific human monoclonal antibody, in healthy adults. Clin Microbiol Infect 25:629.e1–629.e6. https://doi.org/10.1016/j.cmi.2018.08.004.
17. Pennini ME, De Marco A, Pelletier M, Bonnell J, Cvitkovic R, Beltramello M, Cameroni E, Bianchi S, Zatta F, Zhao W, Xiao X, Camara MM, DiGiandomenico A, Semenova E, Lanzavecchia A, Warrener P, Suzich J, Wang Q, Corti D, Stover CK. 2017. Immune stealth-driven O2 serotype prevalence and potential for therapeutic antibodies against multidrug resistant *Klebsiella pneumoniae*. Nat Commun 8:1991. https://doi.org/10.1038/s41467-017-02223-7.
18. Magill SS, Edwards JR, Bamberg W, Beldavs ZG, Dumyati G, Kainer MA, Lynfield R, Maloney M, McAllister-Hollod L, Nadle J, Ray SM, Thompson DL, Wilson LE, Fridkin SK, Emerging Infections Program Healthcare-Associated I. Antimicrobial Use Prevalence Survey Team. 2014. Multistate point-prevalence survey of health care-associated infections. N Engl J Med 370:1198–1208. https://doi.org/10.1056/NEJMoa1306801.
19. Micozzi A, Gentile G, Minotti C, Cartoni C, Capria S, Ballaro D, Santilli S, Pacetti E, Grammatico S, Bucaneve G, Foa R. 2017. Carbapenem-resistant *Klebsiella pneumoniae* in high-risk haematological patients: factors favouring spread, risk factors and outcome of carbapenem-resistant *Klebsiella pneumoniae* bacteremias. BMC Infect Dis 17:203. https://doi.org/10.1186/s12879-017-2297-9.
20. Deleo FR, Chen L, Porcella SF, Martens CA, Kobayashi SD, Porter AR, Chavda KD, Jacobs MR, Mathema B, Olsen RJ, Bonomo RA, Musser JM, Kreiswirth BN. 2014. Molecular dissection of the evolution of carbapenem-resistant multilocus sequence type 258 *Klebsiella pneumoniae*. Proc Natl Acad Sci U S A 111:4988–4993. https://doi.org/10.1073/pnas.1321364111.
21. Habets MN, van Selm S, van der Gaast-de Jongh CE, Diavatopoulos DA, de Jonge MI. 2017. A novel flow cytometry-based assay for the quantification of antibody-dependent pneumococcal agglutination. PLoS One 12:e0170884. https://doi.org/10.1371/journal.pone.0170884.
22. Diago-Navarro E, Chen L, Passet V, Burack S, Ulacia-Hernando A, Kodiyanplakkal RP, Levi MH, Brisse S, Kreiswirth BN, Fries BC. 2014. Carbapenem-resistant *Klebsiella pneumoniae* exhibit variability in capsular polysaccharide and capsule associated virulence traits. J Infect Dis 210:803–813. https://doi.org/10.1093/infdis/jiu157.
23. Satlin MJ, Chen L, Patel G, Gomez-Simmonds A, Weston G, Kim AC, Seo SK, Rosenthal ME, Sperber SJ, Jenkins SG, Hamula CL, Uhlemann AC, Levi MH, Fries BC, Tang YW, Juretschko S, Rojtman AD, Hong T, Mathema B, Jacobs MR, Walsh TJ, Bonomo RA, Kreiswirth BN. 2017. Multicenter clinical and molecular epidemiological analysis of bacteremia due to carbapenem-resistant *Enterobacteriaceae* (CRE) in the CRE epicenter of the United States. Antimicrob Agents Chemother 61:e02349-16. https://doi.org/10.1128/AAC.02349-16.
24. Wyres KL, Gorrie C, Edwards DJ, Wertheim HFL, Hsu LY, Van Kinh N, Zadoks R, Baker S, Holt KE. 2015. Extensive capsule locus variation and large-scale genomic recombination within the *Klebsiella pneumoniae* clonal group 258. Genome Biol Evol 7:1267–1279. https://doi.org/10.1093/gbe/evv062.
25. Xiong H, Carter RA, Leiner IM, Tang YW, Chen L, Kreiswirth BN, Pamer EG. 2015. Distinct contributions of neutrophils and CCR2+ monocytes to pulmonary clearance of different *Klebsiella pneumoniae* strains. Infect Immun 83:3418–3427. https://doi.org/10.1128/IAI.00678-15.
26. Diago-Navarro E, Calatayud-Baselga I, Sun D, Khairallah C, Mann I, Ulacia-Hernando A, Sheridan B, Shi M, Fries BC. 2017. Antibody-based immunotherapy to treat and prevent infection with hypervirulent *Klebsiella pneumoniae*. Clin Vaccine Immunol 24:e00456-16. https://doi.org/10.1128/CVI.00456-16.
27. Malachowa N, Kobayashi SD, Porter AR, Freedman B, Hanley PW, Lovaglio J, Saturday GA, Gardner DJ, Scott DP, Griffin A, Cordova K, Long D, Rosenke R, Sturdevant DE, Bruno D, Martens C, Kreiswirth BN, DeLeo FR. 2019. Vaccine protection against multidrug-resistant *Klebsiella pneu-*

moniae in a nonhuman primate model of severe lower respiratory tract infection. mBio 10:e02994-19. https://doi.org/10.1128/mBio.02994-19.
28. Xiong H, Keith JW, Samilo DW, Carter RA, Leiner IM, Pamer EG. 2016. Innate lymphocyte/Ly6C(hi) monocyte crosstalk promotes *Klebsiella pneumoniae* clearance. Cell 165:679–689. https://doi.org/10.1016/j.cell.2016.03.017.
29. Beers SA, Glennie MJ, White AL. 2016. Influence of immunoglobulin isotype on therapeutic antibody function. Blood 127:1097–1101. https://doi.org/10.1182/blood-2015-09-625343.
30. Damelang T, Rogerson SJ, Kent SJ, Chung AW. 2019. Role of IgG3 in infectious diseases. Trends Immunol 40:197–211. https://doi.org/10.1016/j.it.2019.01.005.
31. Goh YS, Grant AJ, Restif O, McKinley TJ, Armour KL, Clark MR, Mastroeni P. 2011. Human IgG isotypes and activating Fcγ receptors in the interaction of *Salmonella enterica* serovar Typhimurium with phagocytic cells. Immunology 133:74–83. https://doi.org/10.1111/j.1365-2567.2011.03411.x.
32. Saylor CA, Dadachova E, Casadevall A. 2010. Murine IgG1 and IgG3 isotype switch variants promote phagocytosis of *Cryptococcus neoformans* through different receptors. J Immunol 184:336–343. https://doi.org/10.4049/jimmunol.0902752.
33. Dillon MJ, Loban RA, Reed DE, Thorkildson P, Pflughoeft KJ, Pandit SG, Brett PJ, Burtnick MN, AuCoin DP. 2016. Contribution of murine IgG Fc regions to antibody binding to the capsule of *Burkholderia pseudomallei*. Virulence 7:691–701. https://doi.org/10.1080/21505594.2016.1176655.
34. Yuan R, Casadevall A, Spira G, Scharff MD. 1995. Isotype switching from IgG3 to IgG1 converts a nonprotective murine antibody to *Cryptococcus neoformans* into a protective antibody. J Immunol 154:1810–1816.
35. Mukherjee J, Scharff MD, Casadevall A. 1992. Protective murine monoclonal antibodies to *Cryptococcus neoformans*. Infect Immun 60:4534–4541. https://doi.org/10.1128/IAI.60.11.4534-4541.1992.
36. Seeberger PH, Pereira CL, Khan N, Xiao G, Diago-Navarro E, Reppe K, Opitz B, Fries BC, Witzenrath M. 2017. A semi-synthetic glycoconjugate vaccine candidate for carbapenem-resistant *Klebsiella pneumoniae*. Angew Chem Int Ed Engl 56:13973–13978. https://doi.org/10.1002/anie.201700964.
37. Kozel TR, Murphy WJ, Brandt S, Blazar BR, Lovchik JA, Thorkildson P, Percival A, Lyons CR. 2004. mAbs to *Bacillus anthracis* capsular antigen for immunoprotection in anthrax and detection of antigenemia. Proc Natl Acad Sci U S A 101:5042–5047. https://doi.org/10.1073/pnas.0401351101.
38. Casadevall A, Scharff MD. 1991. The mouse antibody response to infection with *Cryptococcus neoformans*: VH and VL usage in polysaccharide binding antibodies. J Exp Med 174:151–160. https://doi.org/10.1084/jem.174.1.151.
39. Cooper LJ, Schimenti JC, Glass DD, Greenspan NS. 1991. H chain C domains influence the strength of binding of IgG for streptococcal group A carbohydrate. J Immunol 146:2659–2663.
40. Klaus T, Bzowska M, Kulesza M, Kabat AM, Jemioła-Rzemińska M, Czaplicki D, Makuch K, Jucha J, Karabasz A, Bereta J. 2016. Agglutinating mouse IgG3 compares favourably with IgMs in typing of the blood group B antigen: functionality and stability studies. Sci Rep 6:30938. https://doi.org/10.1038/srep30938.
41. Greenspan NS, Monafo WJ, Davie JM. 1987. Interaction of IgG3 anti-streptococcal group A carbohydrate (GAC) antibody with streptococcal group A vaccine: enhancing and inhibiting effects of anti-GAC, anti-isotypic, and anti-idiotypic antibodies. J Immunol 138:285–292.
42. Yoo EM, Wims LA, Chan LA, Morrison SL. 2003. Human IgG2 can form covalent dimers. J Immunol 170:3134–3138. https://doi.org/10.4049/jimmunol.170.6.3134.
43. DeLeo FR, Kobayashi SD, Porter AR, Freedman B, Dorward DW, Chen L, Kreiswirth BN. 2017. Survival of carbapenem-resistant *Klebsiella pneumoniae* sequence type 258 in human blood. Antimicrob Agents Chemother 61:e02533-16. https://doi.org/10.1128/AAC.02533-16.
44. Klaus T, Bereta J. 2018. CH2 domain of mouse IgG3 governs antibody oligomerization, increases functional affinity to multivalent antigens and enhances hemagglutination. Front Immunol 9:1096. https://doi.org/10.3389/fimmu.2018.01096.
45. Neuberger MS, Rajewsky K. 1981. Activation of mouse complement by monoclonal mouse antibodies. Eur J Immunol 11:1012–1016. https://doi.org/10.1002/eji.1830111212.
46. Lilienthal GM, Rahmoller J, Petry J, Bartsch YC, Leliavski A, Ehlers M. 2018. Potential of murine IgG1 and human IgG4 to inhibit the classical complement and Fcγ receptor activation pathways. Front Immunol 9:958. https://doi.org/10.3389/fimmu.2018.00958.
47. Kobayashi SD, Porter AR, Dorward DW, Brinkworth AJ, Chen L, Kreiswirth BN, DeLeo FR. 2016. Phagocytosis and killing of carbapenem-resistant ST258 *Klebsiella pneumoniae* by human neutrophils. J Infect Dis 213:1615–1622. https://doi.org/10.1093/infdis/jiw001.
48. Hawk CS, Coelho C, Oliveira DSL, Paredes V, Albuquerque P, Bocca AL, Correa Dos Santos A, Rusakova V, Holemon H, Silva-Pereira I, Felipe MSS, Yagita H, Nicola AM, Casadevall A. 2019. Integrin beta1 promotes the interaction of murine IgG3 with effector cells. J Immunol 202:2782–2794. https://doi.org/10.4049/jimmunol.1701795.
49. Cano V, March C, Insua JL, Aguilo N, Llobet E, Moranta D, Regueiro V, Brennan GP, Millan-Lou MI, Martin C, Garmendia J, Bengoechea JA. 2015. *Klebsiella pneumoniae* survives within macrophages by avoiding delivery to lysosomes. Cell Microbiol 17:1537–1560. https://doi.org/10.1111/cmi.12466.
50. Wang J, Shao Y, Wang W, Li S, Xin N, Xie F, Zhao C. 2017. Caspase-11 deficiency impairs neutrophil recruitment and bacterial clearance in the early stage of pulmonary *Klebsiella pneumoniae* infection. Int J Med Microbiol 307:490–496. https://doi.org/10.1016/j.ijmm.2017.09.012.
51. Codo AC, Saraiva AC, Dos Santos LL, Visconde MF, Gales AC, Zamboni DS, Medeiros AI. 2018. Inhibition of inflammasome activation by a clinical strain of *Klebsiella pneumoniae* impairs efferocytosis and leads to bacterial dissemination. Cell Death Dis 9:1182. https://doi.org/10.1038/s41419-018-1214-5.
52. Georgel P, Radosavljevic M, Macquin C, Bahram S. 2011. The non-conventional MHC class I MR1 molecule controls infection by *Klebsiella pneumoniae* in mice. Mol Immunol 48:769–775. https://doi.org/10.1016/j.molimm.2010.12.002.
53. ten Hagen TL, van Vianen W, Savelkoul HF, Heremans H, Buurman WA, Bakker-Woudenberg IA. 1998. Involvement of T cells in enhanced resistance to *Klebsiella pneumoniae* septicemia in mice treated with liposome-encapsulated muramyl tripeptide phosphatidylethanolamine or gamma interferon. Infect Immun 66:1962–1967. https://doi.org/10.1128/IAI.66.5.1962-1967.1998.
54. Hickman-Davis JM, O'Reilly P, Davis IC, Peti-Peterdi J, Davis G, Young KR, Devlin RB, Matalon S. 2002. Killing of *Klebsiella pneumoniae* by human alveolar macrophages. Am J Physiol Lung Cell Mol Physiol 282:L944–L956. https://doi.org/10.1152/ajplung.00216.2001.
55. Ivin M, Dumigan A, de Vasconcelos FN, Ebner F, Borroni M, Kavirayani A, Przybyszewska KN, Ingram RJ, Lienenklaus S, Kalinke U, Stoiber D, Bengoechea JA, Kovarik P. 2017. Natural killer cell-intrinsic type I IFN signaling controls *Klebsiella pneumoniae* growth during lung infection. PLoS Pathog 13:e1006696. https://doi.org/10.1371/journal.ppat.1006696.
56. Murakami T, Hatano S, Yamada H, Iwakura Y, Yoshikai Y. 2016. Two types of interleukin 17A-producing γδ T cells in protection against pulmonary infection with *Klebsiella pneumoniae*. J Infect Dis 214:1752–1761. https://doi.org/10.1093/infdis/jiw443.
57. Ye P, Rodriguez FH, Kanaly S, Stocking KL, Schurr J, Schwarzenberger P, Oliver P, Huang W, Zhang P, Zhang J, Shellito JE, Bagby GJ, Nelson S, Charrier K, Peschon JJ, Kolls JK. 2001. Requirement of interleukin 17 receptor signaling for lung CXC chemokine and granulocyte colony-stimulating factor expression, neutrophil recruitment, and host defense. J Exp Med 194:519–527. https://doi.org/10.1084/jem.194.4.519.
58. Ye P, Garvey PB, Zhang P, Nelson S, Bagby G, Summer WR, Schwarzenberger P, Shellito JE, Kolls JK. 2001. Interleukin-17 and lung host defense against *Klebsiella pneumoniae* infection. Am J Respir Cell Mol Biol 25:335–340. https://doi.org/10.1165/ajrcmb.25.3.4424.
59. Kerr AR, Paterson GK, Riboldi-Tunnicliffe A, Mitchell TJ. 2005. Innate immune defense against pneumococcal pneumonia requires pulmonary complement component C3. Infect Immun 73:4245–4252. https://doi.org/10.1128/IAI.73.7.4245-4252.2005.
60. Mueller-Ortiz SL, Drouin SM, Wetsel RA. 2004. The alternative activation pathway and complement component C3 are critical for a protective immune response against *Pseudomonas aeruginosa* in a murine model of pneumonia. IAI 72:2899–2906. https://doi.org/10.1128/IAI.72.5.2899-2906.2004.
61. Tian H, Weber S, Thorkildson P, Kozel TR, Pirofski LA. 2009. Efficacy of opsonic and nonopsonic serotype 3 pneumococcal capsular polysaccharide-specific monoclonal antibodies against intranasal challenge with *Streptococcus pneumoniae* in mice. Infect Immun 77:1502–1513. https://doi.org/10.1128/IAI.01075-08.
62. Doyle CR, Moon JY, Daily JP, Wang T, Pirofski LA. 2018. A capsular polysaccharide-specific antibody alters *Streptococcus pneumoniae* gene expression during nasopharyngeal colonization of mice. Infect Immun 86:e00300-18. https://doi.org/10.1128/IAI.00300-18.
63. Miller WG, Leveau JH, Lindow SE. 2000. Improved *gfp* and *inaZ* broad-

host-range promoter-probe vectors. Mol Plant Microbe Interact 13:1243–1250. https://doi.org/10.1094/MPMI.2000.13.11.1243.

64. Mitsi E, Roche AM, Reine J, Zangari T, Owugha JT, Pennington SH, Gritzfeld JF, Wright AD, Collins AM, van Selm S, de Jonge MI, Gordon SB, Weiser JN, Ferreira DM. 2017. Agglutination by anti-capsular polysaccharide antibody is associated with protection against experimental human pneumococcal carriage. Mucosal Immunol 10:385–394. https://doi.org/10.1038/mi.2016.71.
65. Varshney AK, Wang X, Cook E, Dutta K, Scharff MD, Goger MJ, Fries BC. 2011. Generation, characterization, and epitope mapping of neutralizing and protective monoclonal antibodies against staphylococcal enterotoxin B-induced lethal shock. J Biol Chem 286:9737–9747. https://doi.org/10.1074/jbc.M110.212407.
66. Marim FM, Silveira TN, Lima DS, Jr, Zamboni DS. 2010. A method for generation of bone marrow-derived macrophages from cryopreserved mouse bone marrow cells. PLoS One 5:e15263. https://doi.org/10.1371/journal.pone.0015263.
67. Huffnagle GB, Lipscomb MF, Lovchik JA, Hoag KA, Street NE. 1994. The role of $CD4^+$ and $CD8^+$ T cells in the protective inflammatory response to a pulmonary cryptococcal infection. J Leukoc Biol 55:35–42. https://doi.org/10.1002/jlb.55.1.35.